Pergamon

0042-6989(94)00196-0

Vision Res. Vol. 35, No. 7, pp. 915–924, 1995

0042-6989/95 $9.50 + 0.00

Measuring the Spatial Frequency Selectivity of Second-order Texture Mechanisms

ANNE SUTTER,*§ GEORGE SPERLING,† CHARLES CHUBB‡

Received 3 June 1992; in revised form 29 July 1993; in final form 2 August 1994

Recent investigations of texture and motion perception suggest two early filtering stages: an initial stage of selective linear filtering followed by rectification and a second stage of linear filtering. Here we demonstrate that there are differently scaled second-stage filters, and we measure their contrast modulation sensitivity as a function of spatial frequency. Our stimuli are Gabor modulations of a suprathreshold, bandlimited, isotropic carrier noise. The subjects' task is to discriminate between two possible orientations of the Gabor. Carrier noises are filtered into four octave-wide bands, centered at $m = 2$, 4, 8, and 16 c/deg. The Gabor test signals are $w = 0.5$, 1, 2, 4 and 8 c/deg. The threshold modulation of the test signal is measured for all 20 combinations of m and w. For each carrier frequency m, the Gabor test frequency w to which subjects are maximally sensitive appears to be approximately 3–4 octaves below m. The consistent $m \times w$ interaction suggests that each second-stage spatial filter may be differentially tuned to a particular first-stage spatial frequency. The most sensitive combination is a second-stage filter of 1 c/deg with first-stage inputs of 8–16 c/deg. We conclude that second-order texture perception appears to utilize multiple channels tuned to spatial frequency and orientation, with channels tuned to low modulation frequencies appearing to be best served by carrier frequencies 8 to 16 times higher than the modulations they are tuned to detect.

Texture segregation Second-order mechanisms Spatial Frequency

INTRODUCTION

A number of recent studies of texture perception have demonstrated the importance of spatial frequency content in determining the perceived segregation of texture regions. Many of these studies have demonstrated the effectiveness of explanations of texture segregation based on the outputs of orientation and spatial frequency selective linear analyzers, followed directly by decision processes (Bovik, Clark & Geisler, 1987, 1990; Caelli, 1988; Nothdurft, 1985a, b; Turner, 1986; Sutter, Beck & Graham, 1989; see also, Graham 1989). We call this kind of mechanism "first-order" texture perception. It is illustrated in Fig. 1a, which shows the optical input being passed through an array of spatial-frequency- and orientation selective linear spatial filters. The contribution of each filter to a particular detection or discrimination task is determined by a task-dependent weight. The weighted filter outputs simply add and, if at any time the absolute value of the sum exceeds a threshold, detection is signaled.

This deliberately simplified model of first-order texture perception omits much: explicit considerations of how filter weights are determined (i.e., according to filter type and location), considerations of more complex combinations of filter outputs (e.g. probability summation, Quick summation), quantum statistics of the source, internal noise, and so on. Nevertheless, it has been obvious to a growing number of investigators that theories of texture segregation exclusively based on the outputs of a single stage of linear filters followed by a decision mechanism often fail to explain completely perceived texture segregation (Chubb & Sperling, 1988; Rubenstein & Sagi, 1989; Malik & Perona, 1990; Bergen & Landy, 1991). To account for these inadequacies, recent theories have proposed further stages of processing after the initial stage of linear filtering (Chubb & Sperling, 1988, 1989; Graham, Beck & Sutter, 1989, 1992; Grossberg & Mingolla, 1985; Landy & Bergen, 1989, 1991; Victor, 1988; Victor & Conte, 1987, 1989a, b.) Most promising is the addition of a second path for texture perception, one in which the output of the first-stage filters is rectified and passed through a second-stage of linear filters before the decision process (Fig. 1b, c). (By rectification we mean any point-wise, monotonic transformation of the absolute value of

*Department of Psychology, Loyola University, 6525 North Sheridan Road, Chicago, IL 60626, U.S.A.
†Department of Cognitive Science, University of California, Irvine, CA 92717, U.S.A.
‡Department of Psychology, Rutgers University, New Brunswick, NJ 08903, U.S.A.
§To whom all correspondence should be addressed [*Email* asutter@luc.edu].

contrast; i.e. a transformation that treats positive and negative values of contrast symmetrically—absolute value, square etc.) Evidence for such a "second-order" process of texture perception is derived from stimuli that are judged by humans to have highly visible texture patterns, yet which manifest no such patterns to any simple linear-filters-plus-decision model, i.e. to first-order texture mechanisms. We consider two illustrative examples.

Graham, Sutter and Venkatesan (1993) and Malik and Perona (1990) use stimuli in which the elements comprising a texture are "balanced", i.e. the space-averaged luminance of each element is equal to the luminance of the background. When such elements are used to compose a larger texture pattern, the pattern cannot be detected by any linear filter whose spatial scale is on the order of the pattern itself because the individual elements are invisible to that filter. Chubb and Sperling (1988, 1989, 1991) used random textures arranged into drift-balanced stimuli—that is, stimuli that have equal expected Fourier energy at all orientations. Chubb and Sperling proved that pattern orientation in drift-balanced stimuli cannot be discriminated by linear-filter-plus-detection models. Chubb and Sperling (1988) and Graham, Beck and Sutter (1992) observe that a two-stage model that contains an initial stage of linear filtering followed by rectification and a second-stage of filtering (e.g. Fig. 1b) could capture the information that appears to be accessible to humans but inaccessible to a single filter-stage system.

In the experiment reported here, we measure the basic properties of the proposed second-stage filters—their modulation sensitivity as a function of spatial frequency. The stimulus designed to excite the second-stage filters is a two-dimensional Gabor pattern (Fig. 2). If the Gabor were a pattern of amplitude modulation imposed on a field of uniform luminance (Fig. 2a), it would be visible to a single-stage-linear-filter-plus-detection system. To insure that the orientation of the Gabor pattern cannot be discriminated by a first-order mechanism, it is imposed on a field of random visual noise (Fig. 2c; cf. Chubb & Sperling, 1988; Jamar & Koenderink, 1985). To determine the contrast modulation sensitivity of the second-stage system, we obtained amplitude modulation thresholds for Gabor modulations of two-dimensional, suprathreshold, spatially bandlimited carrier noise. The subjects' task was to identify the orientation of the Gabor modulation.

By appropriately choosing the spatial frequencies of the Gabor modulation and carrier noise, it is possible to construct a stimulus that contains no suprathreshold spatial frequency components at the spatial frequencies of the Gabor function, thereby rendering it invisible to a second-stage system. This stimulus contains no suprathreshold spatial frequency components at the spatial frequencies of the Gabor modulation when the spatial frequency of the Gabor is sufficiently lower than the spatial frequencies in the carrier noise. A stimulus of this kind can be constructed by multiplying together (convolving in frequency space) a Gabor function and a carrier whose power spectrum is strictly bandlimited. Because the resulting stimulus contains no significant frequency components at the frequency of the Gabor function, no single stage of linear filtering can signal either the presence or the spatial orientation of the Gabor. A second stage of linear filtering could respond to the Gabor modulation by summing over the rectified outputs of many first-stage filters.

In an earlier study, Jamar and Koenderink (1985) measured amplitude modulation thresholds for one-dimensional sinusoidal modulations of noise carriers of various bandwidths around a fixed central frequency. They found that modulation thresholds rose with the spatial frequency of the modulator, and that the visual system operated with the same efficiency, regardless of the bandwidth of the carrier noise on which the modulations were impressed. They interpreted their results to mean that the second-stage filters were not selective with respect to the spatial frequency tuning of the first-stage filters, but used all first-stage outputs with equal efficiency (Fig. 1b). We propose an alternative interpretation: namely that visual sensitivity varies anti symmetrically with spatial frequency around the center of the bands they investigated. As bandwidth increased increased sensitivity for higher frequencies were compensated by decreased sensitivity for lower frequencies, so that overall sensitivity remained constant. Indeed, one of the main results of the research we report here is that the second-stage filters are selective with respect to the tuning of the first-stage filters (Fig. 1c).

Whereas Jamar and Koenderink (1985) measured detection thresholds for modulations of carrier noise with fixed carrier frequency and variable bandwidth, we instead measure detection thresholds for modulations of carrier noises with a fixed bandwidth, but variable center frequency. We employ five spatial frequencies of Gab

FIGURE 1 (*opposite*). Models of texture detection and discrimination tasks. (a) First-order model. The optic input is processed by an array of spatial linear filters varying in spatial frequency (indicated by cross-section of a 2D impulse response), spatial location, orientation specificity, bandwidth, etc. The output of each filter is multiplied by a task-dependent weight, w_i. Weighted outputs are combined (summation is indicated here). The decision box indicates an input/output characteristic, x = input, y = output. The decision component outputs a 1 whenever its input departs from zero by a threshold amount, otherwise its output is zero. (b) Single-channel second-order model. This pathway, which is assumed to exist in parallel with (a), rectifies the outputs of the first-stage filters before combining them. Rectification is any pointwise monotonic transformation of the absolute value of contrast; the absolute value is illustrated. A second-stage filter operates on the rectified, combined outputs prior to the detection stage. Different second-stage filters are possible, only one is shown. (c) Multichannel second-order model. The multichannel model differs from the single-channel model in that different classes of second-stage filters (channels) receive differently weighted inputs w_{ij} from the first-stage filters.

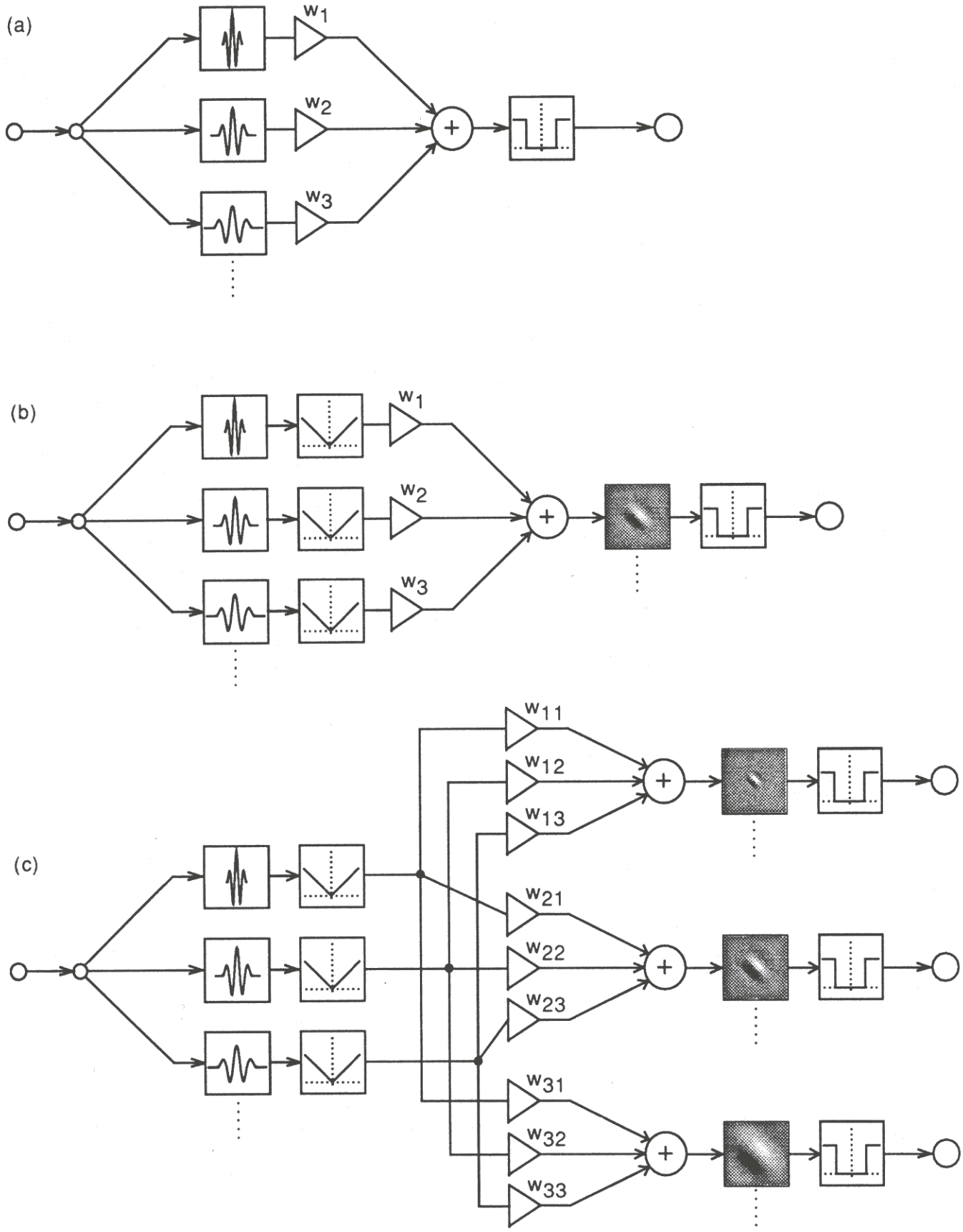

FIGURE 1—*caption opposite.*

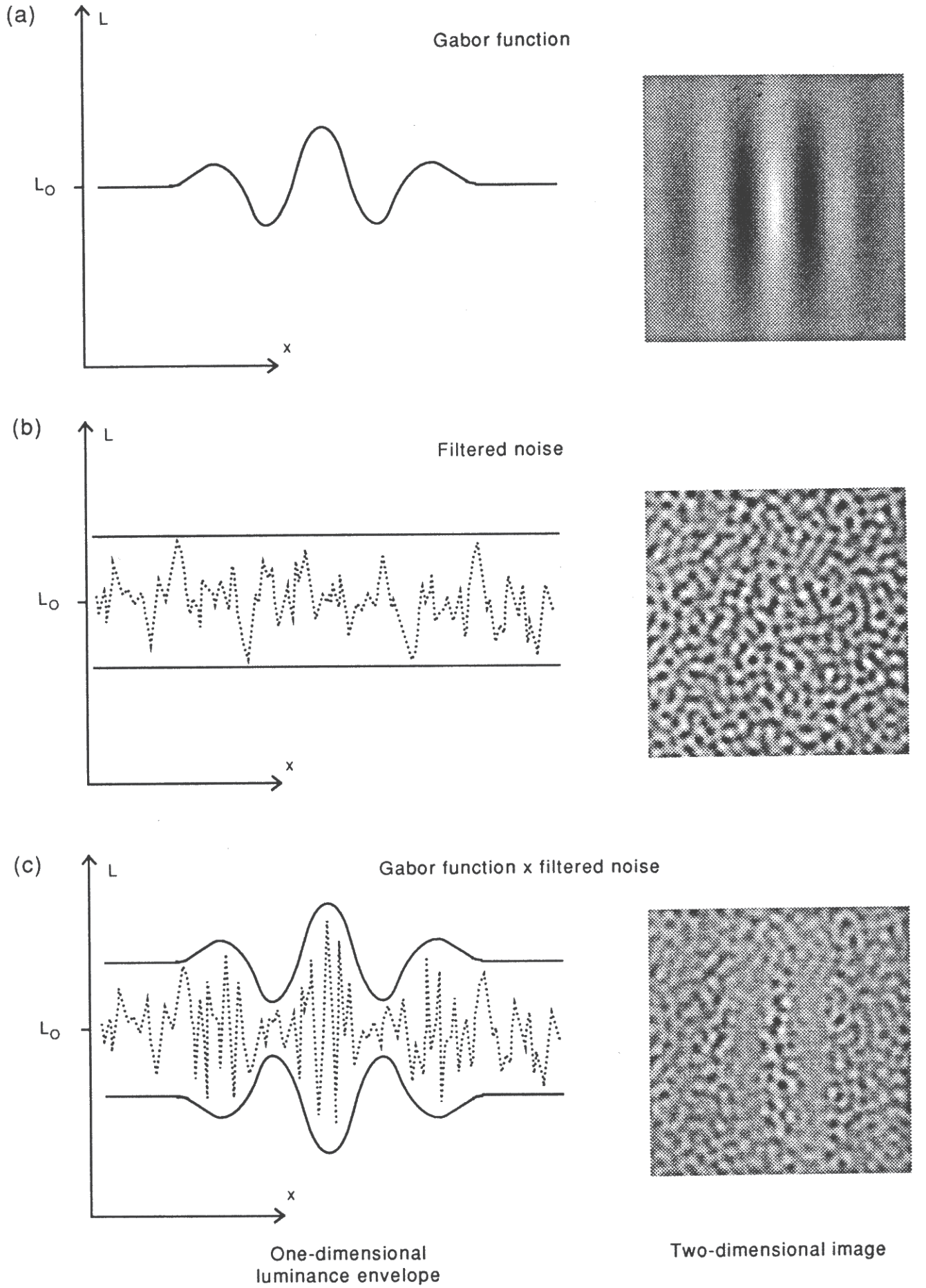

FIGURE 2—*caption opposite.*

modulation (0.5, 1, 2, 4 and 8 c/deg) and bandlimited noise carriers centered at four different frequencies (2, 4, 8 and 16 c/deg), in order to determine the modulation sensitivity function of the second-stage system and its frequency selectivity with respect to the first-stage filters. Most of the combinations of carrier frequency and modulator are shown in Fig. 3.

METHOD

Apparatus

The stimuli were presented on a US Pixel PX-15 monochrome monitor using an Adage RDS 3000 image display system. The mean luminance was approximately 40 cd/m^2; the refresh rate was 60 Hz, noninterlaced. The resolution of the display was 256 × 256 pixels. Elaborate precautions were taken to achieve luminance linearization. Separate lookup tables were constructed, one for the two lowest, and one for the two highest frequencies of carrier noise to control the conversion of the digital representations of stimuli to voltages (i.e. luminances).

Stimuli

Carrier noise. The stimuli were constructed on a digital computer using specially designed applications programs and the HIPS image-processing software package (Landy, Cohen & Sperling, 1984). Stimuli consisted of isotropic visual noise fields whose amplitudes were modulated by Gabor functions. To create a noise field, random numbers from a uniform density function (mean = 0) were associated with points in the complex Fourier domain. The noise field was digitally filtered by an ideal filter (perfect transmission within a band, zero transmission outside the band) into an octave-wide band with center-frequency μ where, on each trial, μ was one of 2, 4, 8, or 16 c/deg. Pixel values above or below 3σ from the mean were truncated. Then the noise images were scaled to produce luminance values spanning the maximum range of the monitor.

Gabor modulation. The filtered noise field was multiplied by a spatial function G of the following form

$$G(x, y) = 1 + \alpha \cdot \exp\left[\frac{-(x - x_{cntr})^2 - (y - y_{cntr})^2}{2\sigma_\omega^2}\right] \times \cos(2\pi\omega(\gamma x + (1 - \gamma)y) + \rho),$$

where G is a Gabor function plus 1 (Fig. 2b). In order to insure that G was everywhere nonnegative, the amplitude α was restricted to the interval (0, 1). On any given trial, the spatial frequency ω of the grating windowed in G was one of 0.5, 1, 2, 4, or 8 c/deg. The standard deviation σ_ω of the circular Gaussian window of the Gabor function was 0.4 cycles of the windowed grating for gratings of frequencies $\omega = 1$, 2, 3, 4, and 8 c/deg, yielding a spatial-frequency half-amplitude full-bandwidth of approximately 0.6 octaves. For 0.5 c/deg gratings, technical constraints compelled us to use a broader band Gabor function: specifically, for $\omega = 0.5$ c/deg, the standard deviation σ_ω of the Gaussian window was 0.225 cycles of the windowed grating, yielding a spatial-frequency half-amplitude full-bandwidth of approximately 1.1 octaves. The center of the Gabor function window, (x_{cntr}, y_{cntr}), was fixed in the middle of the visual field. The parameter γ, governing the orientation of the grating windowed in the Gabor function, was randomly either 0 or 1 from trial to trial, making the orientation of the grating vertical or horizontal with equal probability. The phase ρ of the Gabor function grating was randomly either 0 or $\pi/2$ on any given trial.

The two primary independent variables were μ (the center spatial frequency of the carrier noise) and ω (the spatial frequency of the Gabor modulation function). ω ranged over the values 0.5, 1, 2, 4, and 8 c/deg; μ ranged over the values 2, 4, 8, and 16 c/deg. Thus there were 20 stimulus conditions in all (12 of them are shown in Fig. 3). This complete crossing of carrier and modulation frequencies produced six stimuli that contain Fourier components at the spatial frequency of the Gabor modulation (low frequency carrier modulated by high frequency Gabor). The amplitude of modulation, α, was controlled by a staircase in the manner described below.

A representative set of stimuli with a range of modulation amplitudes and including the complete range of Gabor modulation and carrier noise frequencies was inspected prior to the experiment to check that luminance was properly linearized, and that there indeed was no Fourier energy artifactually introduced at the spatial frequency of the Gabor modulation (that is for stimuli whose computed Fourier spectra did not contain sufficient energy for orientation discrimination). These checks were accomplished by viewing the stimuli from a variety of distances, and or by blurring. It was found that the Gabor modulation was never visible unless the carrier noise in the stimulus was also visible. That is, there were no Fourier artifacts; Gabors were visible only when second-order (nonFourier) information was available. Of course, the subclass of six stimuli composed

FIGURE 2 (*opposite*). Gabor modulations. (a) Left: one-dimensional cross section of a two-dimensional Gabor modulation of a uniform field of luminance L_0. The abscissa indicates space x, ordinate indicates luminance $L(x)$. Right: an x, y representation of the 2D Gabor modulation $L(x, y)$. Shading (light or dark) indicates luminance values (greater or smaller) than the background. (b) Left: one-dimensional cross section of a two-dimensional, bandlimited, isotropic noise carrier. The abscissa indicates space x, ordinate indicates luminance $L(x)$. Right: an x, y representation of the 2D noise carrier $L(x, y)$. Shading (light or dark) indicates luminance values (greater or smaller) than the background. (c) Left: Gabor modulation of a noise carrier. Right: an x, y representation of the 2D Gabor modulation of noise. A first-order mechanism can detect the Gabor modulation in pattern (a) but not the Gabor modulation in pattern (c). Detection of (c) requires a second-order mechanism.

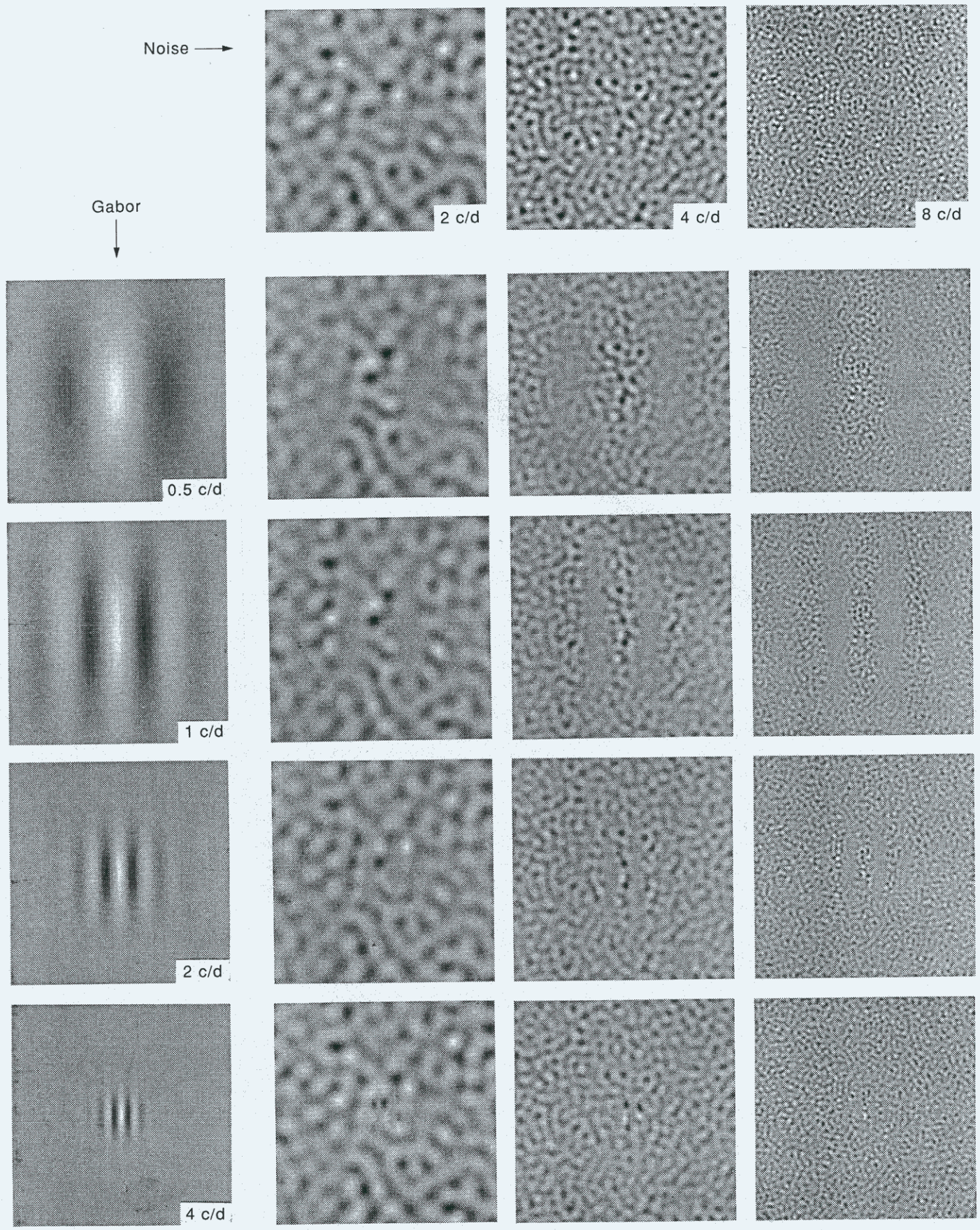

FIGURE 3. Examples of stimuli. Twelve of the 20 combinations of Gabor modulator (left column) and carrier noise (top row). The remaining eight stimulus conditions, composed of combinations including either the 8 c/deg Gabor or the 16 c/deg carrier noise are not shown because of the limitations of photo reproduction. The reproduction process may have altered the appearance of the stimuli shown above.

of high frequency Gabors imposed on low frequency carriers does contain real Fourier energy at the spatial frequency of the Gabor. These stimuli were included in the experiment for completeness of the crossed design but (obviously) were excluded from our analyses of second-order frequency selectivity.

Subjects

Two subjects with normal or corrected-to-normal vision participated in the experiment. Both were highly practiced in psychophysical experiments.

Procedure

The subjects's task was a two alternative forced-choice, indicating for each pattern the orientation (vertical or horizontal) of the Gabor modulation of carrier noise. The subject was seated in a dark room 1.6 m from the monitor screen. Each trial began with a fixation cross in the center of the screen. The subject initiated a trial by pressing a key, after which the following sequence of events occurred: The fixation cross was immediately erased from the screen, which remained blank for 1 sec. The stimulus then appeared for a duration of 500 msec, after which it disappeared and the screen was again blank.. Throughout the experiment, including the intervals during which the screen was blank, the mean luminance of the screen never varied. After the subject responded, a letter "V" or "H" appeared on the screen to indicate his or her response. The subject received feedback in the form of a tone that indicated an incorrect response.

Forty interleaved staircases were used to determine subject's amplitude modulation thresholds (Levitt, 1971). There were 2 staircases for each of the 20 combinations of 4 noise carrier bands and 5 Gabor modulation frequencies, one converging on $P(\text{correct}) = 0.707$, and the other converging on $P(\text{correct}) = 0.794$. The staircases were run until all of them had produced 10 reversals. The last 8 reversals were then averaged to give a threshold estimate. The reported results are the average of the 2 threshold estimates from the 2 staircases for each of the 20 stimuli.

RESULTS AND DISCUSSION

The results of the experiment are shown, for each subject separately, in Fig. 4a–f. The standard errors ranged from 0.5 to 6% amplitude modulation, with most of them falling between 0.75 and 2.0%. Most of the standard errors are not larger than the size of the symbols in Fig. 4. All of the differences between data points that are discussed below are significant, except where noted. Figure 4a, b shows Gabor amplitude modulation sensitivity, the reciprocal of amplitude modulation threshold, as a function of the spatial frequency composition of the carrier noise, for each of the five spatial frequencies of Gabor modulator. Figure 4a, b contains data for the subclass of six stimuli that have Fourier energy at the spatial frequency of the Gabor modulator (i.e. the spatial frequencies in the carrier noise are lower than, or include the spatial frequency of the Gabor modulator). These points are marked with solid squares, and do not appear in the other figures and are not included in the discussion below. We note here that amplitude modulation sensitivity for these subclass stimuli decreases as the frequency of the carrier noise increases to approach the spatial frequency of the Gabor, reflecting decreased Fourier energy in the Gabor, and probably also masking of the (Fourier) Gabor by the carrier.

An interaction is evident between the spatial frequency of the Gabor modulation and the spatial frequency band of the carrier. This can be seen in Fig. 4a, b in the lack of parallelism between the curves. This indicates that although the second-stage filters appear to be broadly tuned (there are no abrupt decreases in sensitivity, ignoring the points marked by solid squares), there is evidence of some selectivity with respect to the spatial frequency components of the carrier noise. We return to this point later.

Figure 4c, d shows amplitude modulation sensitivity, as a function of the spatial frequency of the Gabor modulating signal, for the four carrier noise bands. These graphs represent the modulation sensitivity functions of the second-stage filters. The characteristics of the modulation sensitivity functions are very similar for the two subjects. Both show a peak sensitivity for modulation frequencies of 1 c/deg or lower. The decrease in sensitivity with increasing modulation frequency might be due to the fact that the Gabor patches decreased in size with increasing modulation frequency (as happens when log bandwidth is held constant). Because the Gabor patches were smaller, they may have been more difficult to detect. However, in a pilot experiment in which the size of the Gabor patch was held constant across modulation frequencies, amplitude modulation sensitivity showed a very similar decrease with spatial frequency of the Gabor modulator. Moreover, Jamar and Koenderink (1985), in their experiments involving the detection of sinusoidal amplitude modulations of noise gratings, found that regardless of the number of cycles present in the stimulus, the subjects used only about one modulation cycle for detection. Taken together, these findings make it unlikely that the differences we found in sensitivity to modulation frequency were due to variations in the retinal size of the modulating Gabor patch.

Figure 4c, d also shows, for both subjects, a decrease in sensitivity to 0.5 c/deg modulations for a carrier centered at 16 c/deg, and one subject shows this decrease for a carrier centered at 8 c/deg as well.* For modulation

*Direct comparisons between the 0.5 c/deg and other modulation frequencies are made with a little caution because the 0.5 c/deg modulator had a larger bandwidth than the other modulators (i.e., it contained fewer cycles due to the limited total display area). However, according to Jamar and Koenderink (1985, cited above), one cycle is sufficient to reach maximum sensitivity. Further, the "missing" peripheral cycles would have been of lower contrast than the displayed cycles, so we do not expect that this difference produced any significant changes in threshold.

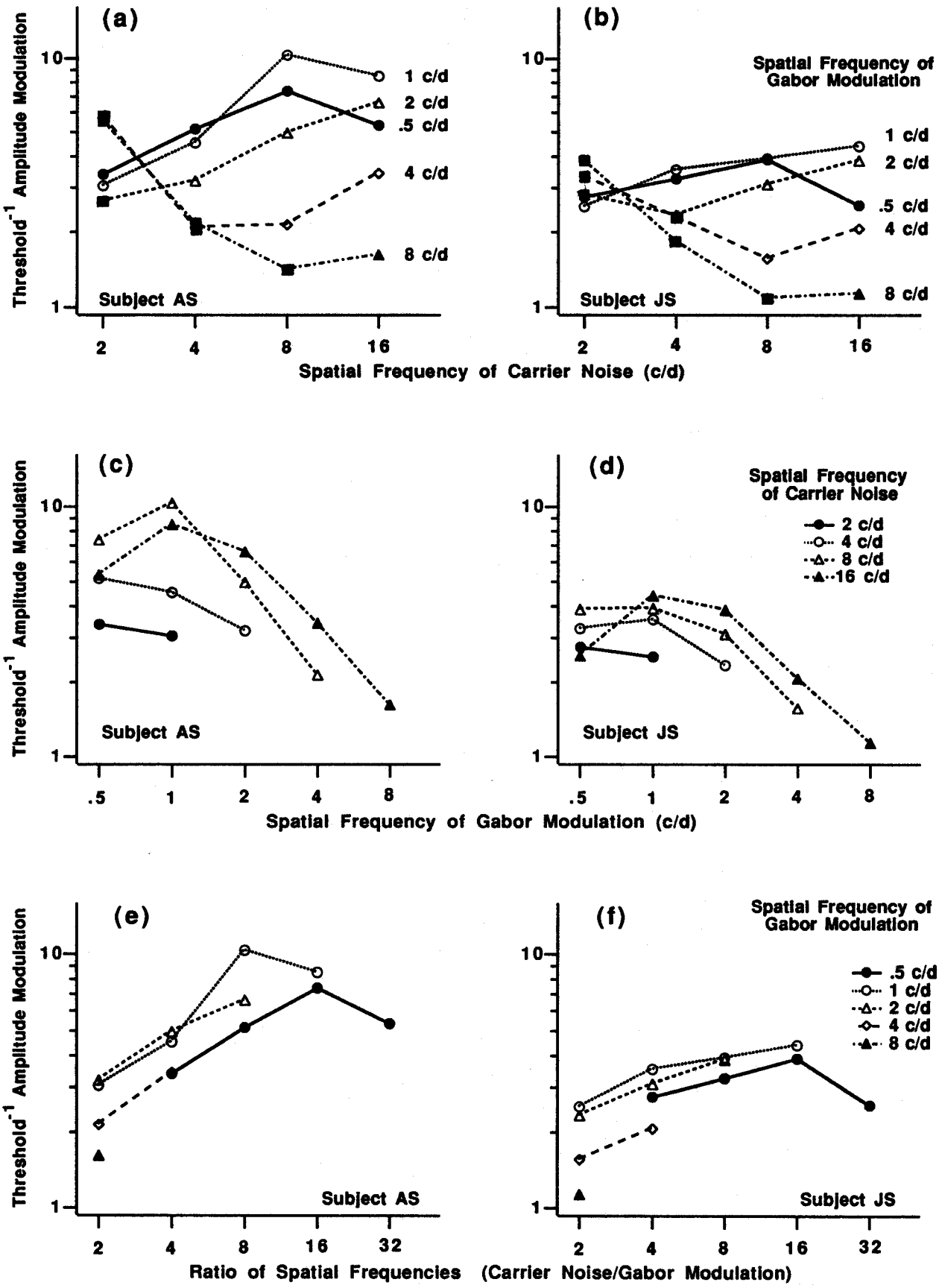

FIGURE 4. Experimental results. Amplitude modulation sensitivity (the reciprocal of amplitude modulation threshold) is plotted as a function of (a, b) the spatial frequency of the carrier noise, (c, d) the spatial frequency of the Gabor modulator, (e, f) the ratio: carrier noise spatial frequency/Gabor modulator spatial frequency, for subjects AS (left column) and JS (right column).

frequencies of 2 c/deg and above, sensitivity is highest when the modulating signals are carried by noise with an octave-wide frequency band centered around 16 c/deg. A crossover occurs at around 1 c/deg, where sensitivity becomes greater for noise carriers centered around 8 c/deg. For both subjects, the differences between the 8 and 16 c/deg carriers are significant at the modulation frequencies of 0.5 and 2 c/deg, but not at 1 c/deg, where the two curves cross over.*

Figure 4e shows the same data that are depicted in Fig. 4a–d. This time, however, amplitude modulation sensitivity is plotted against the ratio of carrier spatial frequency/Gabor modulation spatial frequency. Both subjects show a peak in modulation sensitivity at carrier spatial frequency/Gabor spatial frequency ratio of 8:1 or 16:1. This suggests that the second-stage filters are broadly tuned, scaled replicas of each other, showing a preference with respect to the spatial frequency tuning of their first-stage filters. Second-stage filters tuned to low modulation frequencies appear to show a peak sensitivity to input from first-stage filters tuned to spatial frequencies about three to four octaves higher than the modulation frequency to which the second-stage filters are tuned.

Relation to second-order processing mechanisms

The Carrier Contrast Sensitivity Functions (CCSFs, the curves representing sensitivity as a function of carrier frequency) in Fig. 4a, b are not parallel. However, the simple model of second-order texture perception illustrated in Fig. 1b requires that the CCSFs of Fig. 4a, b be parallel. That is because there is only one set of filters for carrier frequencies, and only one modulator filter, and they are in series. It is essentially a single-channel model, the properties of the channel being defined by the various input filters and weights. Therefore, joint sensitivity to a particular carrier and modulator is the product of the sensitivities to each—the carrier and modulator frequencies are separable. Strictly speaking, a monotonic transformation is permitted on the model's output (to transform the model's internal units to percent correct in a 2AFC task), and parallelism is required only after this transformation. But the curves of Fig 4a, b are not laminar, so no monotonic transformation can make them parallel. Moreover, the simple model also requires the modulator curves of Fig. 4c, d be laminar, another prediction that is violated.

The lack of laminarity in Fig. 4a, e is in contrast to the data of Jamar and Koenderink (1985) who observed approximate parallelism in both their CCSF functions and their modulator functions, an therefore postulated a single-channel mechanism. However, we have already observed that, because of the unique nature of their stimuli (in which only carrier bandwidth, and not carrier center frequency, was varied), parallelism would result from antisymmetric changes in sensitivity above and below their carrier's central frequency.

On the other hand, when in Fig. 4e, f these non-laminar CCSFs (of Fig. 4a, b) are shifted by an amount equal to their modulators, the translated CCSFs become more parallel. Indeed, when the top two data curves in Fig. 4c, d are vertically translated to provide the best superposition of the data, the mean curve-to-curve standard deviation is 0.150. On the other hand, when the 0.5 and 1 c/deg curves of Fig. 4e, f are vertically shifted, the mean residual standard deviation is 0.074, suggesting a better fit. Parallelism after normalization for modulator frequency is just what would be expected if each second-order detector had a unique preference for input frequencies, namely a preference for carrier frequencies at least three to four octaves higher than its own Gabor frequency. Such data suggest a multi-channel model as illustrated in Fig. 1c. Whether there is a practical continuum of second-order filters (in terms of central frequency) or whether a small number of filters well-placed in the frequency domain can capture the data (as in the data of Wilson & Bergen, 1979; Bergen, Wilson & Cowen, 1979) is a question that cannot be answered with only the 20 available data points. However, taking into account the cautions of the footnotes on p. 921 and this page, the data suggest the rejection of a single-channel model (e.g. Fig. 1b). The data are, however, consistent with a multichannel model (e.g. Fig. 1c) for second-order texture perception. Although we can suggest that there are multiple second-order channels to serve a range of spatial frequencies, and that these channels are sufficiently tuned to orientation to discriminate gratings separated by 90 deg, we know very little about their frequency and orientation bandwidths, spatial sampling density, and other salient properties (but see Graham *et al.*, 1993). Similarly, the present study, which uses 2D isotropic noise, does not shed any significant light on the composition of the first stage filters. On the other hand, it is worth noting that the perception of second-order motion-from-texture does *not* require multiple channels for stimuli whose motion is carried by differences only in texture spatial frequency. In this case, the perception of second-order motion-from-texture (unlike perception of second-order texture orientation) is quite adequately explained by a single-channel model (Werkhoven, Sperling & Chubb, 1993). On the other hand,

*Although the bandwidth of the 0.5 c/deg Gabors used in our experiments was larger than the bandwidths used for higher spatial frequency Gabors, this stimulus difference should have no effect on the *crossovers* between curves corresponding to carrier noises of different spatial frequencies. The previous footnote considered the possibility that for a Gabor G of spatial frequency ω, a decrease in the size of G's Gaussian window (corresponding to an increase in bandwidth) might have an effect on the discriminability of G—modulations impressed upon visual noise. However, there is no reason to suppose that changes in the size of G's window would significantly affect the relative discriminabilities of G—modulations impressed upon carrier noises of different spatial frequencies. Thus, even if there were a decrease (or an increase) in sensitivity for 0.5 c/deg modulations of visual noise resulting from a decrease in the size of the Gabor window, we would certainly expect any such change in sensitivity to apply evenhandedly to carrier noises of different spatial frequencies, preserving the crossovers we observe in our data.

discrimination of motion carried by different texture orientations involves two channels (Werkhoven, Sperling & Chubb, 1994).

CONCLUSION

The results of this experiment suggest the existence of a texture segregation mechanism consisting of two stages of linear filters separated by rectification or a similar nonlinearity. Discrimination of different modulation frequencies is served by different second-stage filters, selectively tuned to spatial frequency and orientation. The most sensitive second-stage filter detects modulation frequencies in the neighborhood of 0.5 to 1 c/deg. Second-stage filters appear to be broadly tuned but, relative to their own preferred frequency, they appear to most efficiently utilize the outputs of first-stage filters tuned to carrier frequencies up to three or four octaves higher. That is, second-order texture perception appears to utilize multiple channels that may be best served by carrier frequencies 8 to 16 times higher than the modulation frequencies they are tuned to detect.

REFERENCES

Bergen, J. R. & Landy, M. S. (1991). Computational modeling of visual texture segregation. In Landy, M. S. & Morshon, J. A. (Eds), *Computational models of visual processing*. Cambridge, MA: MIT Press.

Bergen, J. R., Wilson, H. R. & Cowen, J. D. (1979). Further evidence for four mechanisms mediating vision at threshold: Sensitivities to complex gratings and aperiodic stimuli. *Journal of the Optical Society of America, 69*, 1580–1587.

Bovik, A. C., Clark, M. & Geisler, W. S. (1987). Computational texture analysis using localized spatial filtering. *Proceedings of Workshop on Computer Vision*, Miami Beach, FL, Nov. 30–Dec. 2, 1987, pp. 201–206. The IEEE Computer Society Press.

Bovik, A. C., Clark, M. & Geisler, W. S. (1990). Multichannel texture analysis using localized spatial filters. *IEEE Transactions on Pattern Analysis and Machine Intelligence 12*(1), 55–73.

Caelli, T. M. (1988). An adaptive computational model for texture segmentation. *IEEE Transactions on Systems, Man, and Cybernetics, 18*, 1.

Chubb, C. & Sperling, G. (1988). Drift-balanced random stimuli: A general basis for studying non-Fourier motion perception. *Journal of the Optical Society of America A, 5*, 1986–2007.

Chubb, C. & Sperling, G. (1989). Second-order motion perception: Space/time separable mechanisms. *Proceedings: Workshop on Visual Motion*, Irvine, CA, 1987. Washington D.C.: IEEE Computer Society Press, pp. 126–138.

Chubb, C. & Sperling, G. (1991). Texture quilts: Basic tools for studying motion-from-texture. *Journal of Mathematical Psychology, 35*, 411–442.

Graham, N. (1989). *Visual pattern analyzers*. New York: Oxford University Press.

Graham, N., Beck, J. & Sutter, A. (1992). Nonlinear processes in spatial-frequency channel models of perceived texture segregation: Effects of sign and amount of contrast. *Vision Research, 32*, 719–743.

Graham, N., Sutter, A. & Venkatesan, C. (1993). Spatial-frequency- and orientation-selectivity of simple and complex channels in region segregation. *Vision Research, 33*, 1893–1911.

Grossberg, S. & Mingolla, E. (1985). Neural dynamics of perceptual grouping: Textures, boundaries, and emergent features. *Perception & Psychophysics, 38*, 141–171.

Jamar, J. H. T. & Koenderink, J. J. (1985). Contrast detection and detection of contrast modulation for noise gratings. *Vision Research, 25*, 511–521.

Landy, M. S. & Bergen, J. R. (1989). Texture segregation for filtered noise patterns. *Supplement to Investigative Ophthalmology and Visual Science, 30*, 3, 160.

Landy, M. S. & Bergen, J. R. (1991). Texture segregation and orientation gradient. *Vision Research, 31*, 679–691.

Landy, M. S., Cohen, Y. & Sperling, G. (1984). HIPS: Image processing under UNIX. Software and applications. *Behavior Research Methods, Instruments, and Computers, 2*, 199–216.

Levitt, H. (1971). Transformed up-down methods in psychoacoustics. *Journal of Acoustical Society of America, 49*, 467–477.

Malik, J. & Perona, P. (1990). Preattentive texture discrimination with early vision mechanisms. *Journal of the Optical Society of America A, 7*, 923–932.

Nothdurft, H. C. (1985a). Orientation sensitivity and texture segmentation in patterns with different line orientation. *Vision Research, 25*, 551–560.

Nothdurft, H. C. (1985b). Sensitivity for structure gradient in texture discrimination tasks. *Vision Research, 25*, 1957–1968.

Rubenstein, B. S. & Sagi, D. (1989). Spatial variability as a limiting factor in texture discrimination tasks: Implications for performance asymmetries. *Journal of the Optical Society of America, A*, 1632–1643.

Sutter, A., Beck, J. & Graham, N. (1989). Contrast and spatial variables in texture segregation: Testing a simple spatial-frequency channels model. *Perception & Psychophysics, 46*, 312–332.

Turner, M. R. (1986). Texture discrimination by Gabor function. *Biological Cybernetics, 55*, 71–82.

Victor, J. D. (1988). Models for preattentive texture discrimination: Fourier analysis and local feature processing in a unified framework. *Spatial Vision, 3*, 263–280.

Victor, J. D. & Conte, M. (1987). Local and long-range interaction in pattern processing. *Supplement to Investigative Ophthalmology and Visual Science, 28*, 362.

Victor, J. D. & Conte, M. (1989a). Cortical interactions in texture processing: Scale and dynamics. *Visual Neuroscience*, 297–313.

Victor, J. D. & Conte, M. (1989b). What kinds of high-order correlation structure are readily visible? *Investigative Ophthalmology & Visual Science (Suppl.), 30*, 3, 254.

Werkhoven, P., Sperling, G. & Chubb, C. (1993). The dimensional of the computation of motion from texture. *Vision Research*, 463–485.

Werkhoven, P., Sperling, G. & Chubb, C. (1994). Perception of apparent motion between dissimilar gratings: Spatiotemporal properties. *Vision Research, 34*, 2741–2759.

Wilson, H. R. & Bergen, J. R. (1979). A four mechanism model for threshold spatial vision. *Vision Research, 19*, 19–32.

Acknowledgements—This research was supported by a g to G. Sperling from AFOSR, Life Sciences Directorate, Vi Information Processing Program, and by NIMH Applied Cogn Concentration Training Grant 5-T32-M H14267 to A. Sutter.